Figure 1. Detection of v-*fms* and PDGF receptor-related gene fragments in human placenta and thymus DNAs. Hybridization of a v-*fms* probe (A) or a mouse PDGF receptor probe (B) to human placenta (lane 1 and 3) or thymus (lane 2 and 4) DNAs under stringent (50% formamide; lane 1 and 2) or relaxed (30% formamide; lane 3 and 4) hybridization conditions. Arrows indicate the 12-kbp *Eco*RI fragment detected under relaxed conditions by both v-*fms* and mouse PDGF-R probes.

73

λT11

EcoRI   PstI   XbaI   PstI BamHI   EcoRI   1Kbp
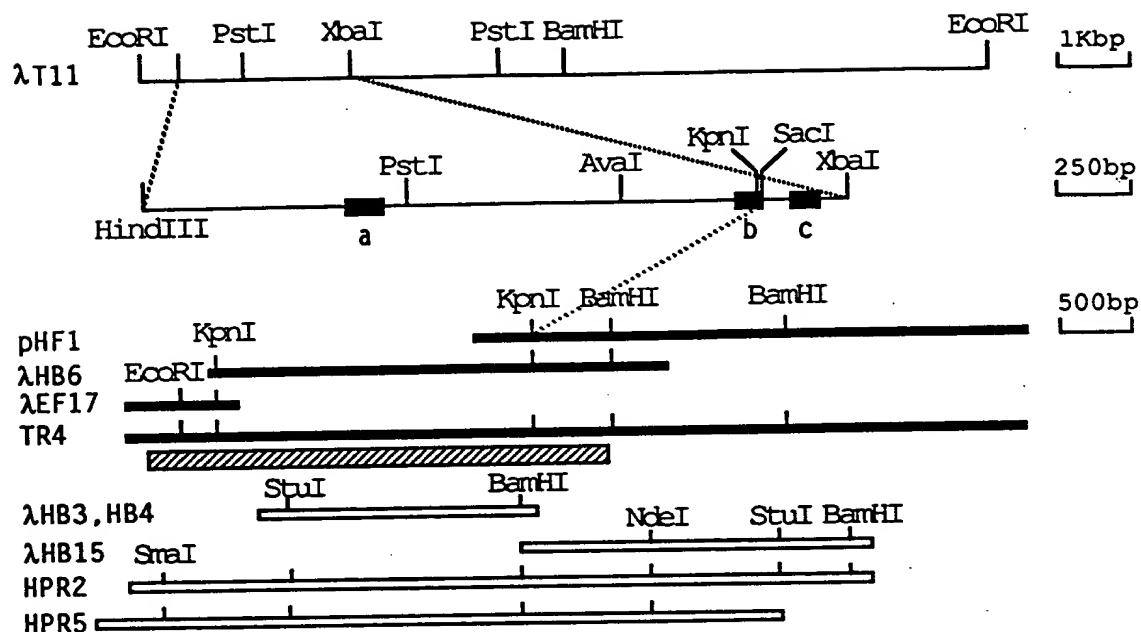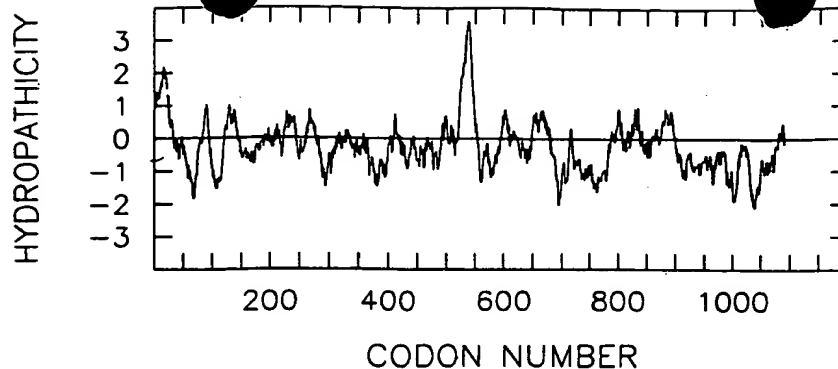
                                              KpnI SacI
                  PstI   AvaI   XbaI   250bp
HindIII   a   b   c

                         KpnI BamHI   BamHI   500bp
pHF1   KpnI
λHB6   EcoRI
λEF17
TR4

λHB3,HB4   StuI   BamHI
                                      NdeI   StuI BamHI
λHB15 SmaI
HPR2
HPR5

Figure 2. Molecular cloning of the λT11 genomic
fragment as well as cDNAs of T11 and PDGF-R
genes. Restriction map of: λT11 genomic clone
(solid lines); T11 cDNA clones (solid bars); and
PDGF-R cDNA clones (open bars). Coding regions
within three fragments, as determined by
nucleotide sequencing analysis, are indicated by
black boxes labeled a, b and c.

Figure 3. See Legend on next page

Figure 3. T11 cDNA nucleotide and predicted
amino acid sequences. Nucleotides are numbered
at the left. The predicted amino acid sequence
of the long open reading frame is shown above the
5   nucleotide sequence. Amino acids are numbered
over the amino acids, starting at the putative
initiation codon. The potential N-terminal
signal sequence is underlined. Potential sites
of N-linked glycosylation are overlined, and
10   cysteine residues are boxed. The putative single
transmembrane region is indicated by a shaded
bar. The potential ATP binding site in the
kinase domain is indicated by circles over Gly at
residues 600, 602 and 605 and Lys at residue
15   627. The putative tyrosine autophosphorylation
site at residue 849 is indicated by *. The
regions of the λT11 genomic sequence defined by
exons a, b and c are underlined. The AATAAA box
close to the polyadenylated 3' end of the cDNA is
20   underlined as well.

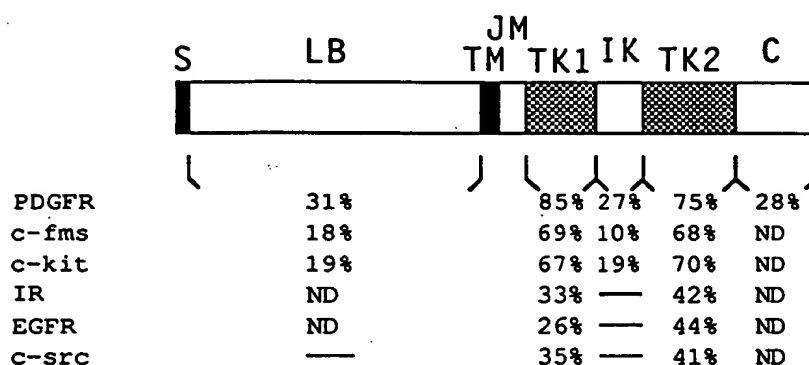|	LB	TM/TK1	IK	TK2	C
PDGFR	31%	85%	27%	75%	28%
c-fms	18%	69%	10%	68%	ND
c-kit	19%	67%	19%	70%	ND
IR	ND	33%	—	42%	ND
EGFR	ND	26%	—	44%	ND
c-src	—	35%	—	41%	ND

Figure 4. Hydropathicity profile and homology with other tyrosine kinases of the T11 receptor-like gene product. A schematic diagram of the predicted protein domains shows the signal sequence (S; black box), ligand binding domain (LB), transmembrane domain (TM; second black box), juxtamembrane domain (JM), tyrosine kinase domains (TK1, TK2; hatched boxes), inter-kinase domain (IK) and carboxyl terminus (C). The hydropathicity profile was calculated by the method of Kyte and Doolittle (46). The homology percentages shown refer to identical amino acids within each respective domain. Abbreviations: IR, insulin receptor; EGF-R, epidermal growth factor receptor; ND, not determined.
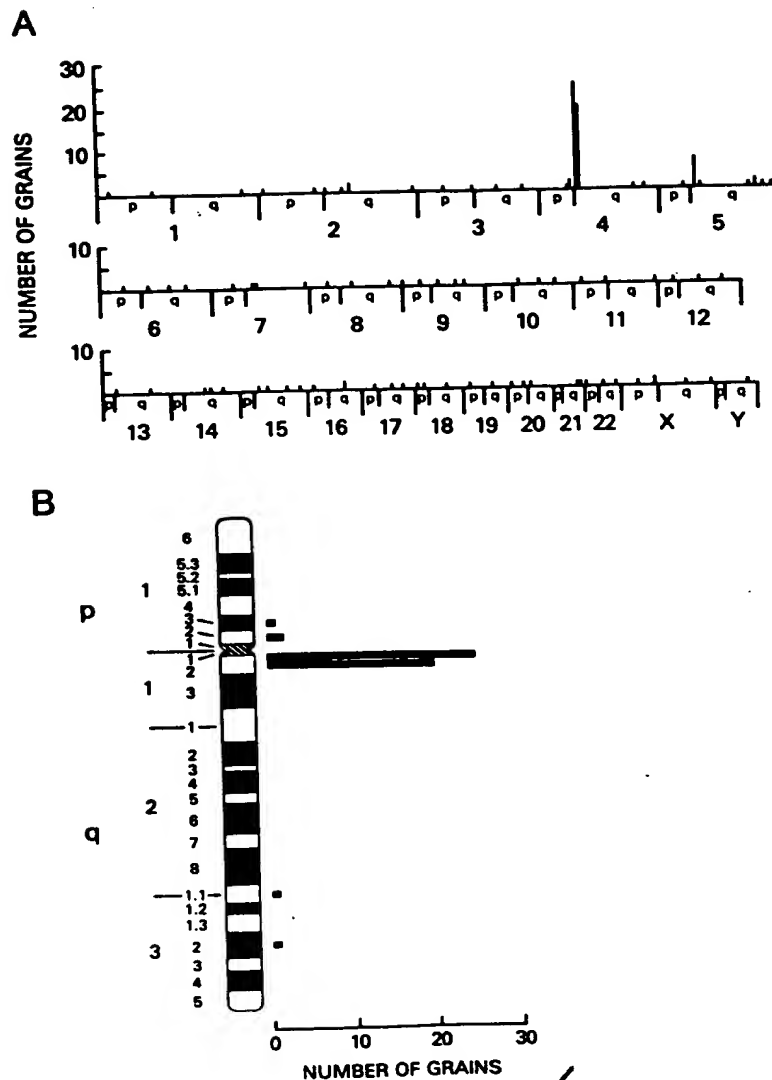
Figure 5. Chromosome mapping of the T11 gene.
(A) Distribution of silver grains on normal human
chromosomes by *in situ* hybridization with pT11-P
probe (clone of the 3.6-kbp *Pst*I genomic fragment)
(see Fig. 1). (B) Distribution of grains on
chromosome 4.

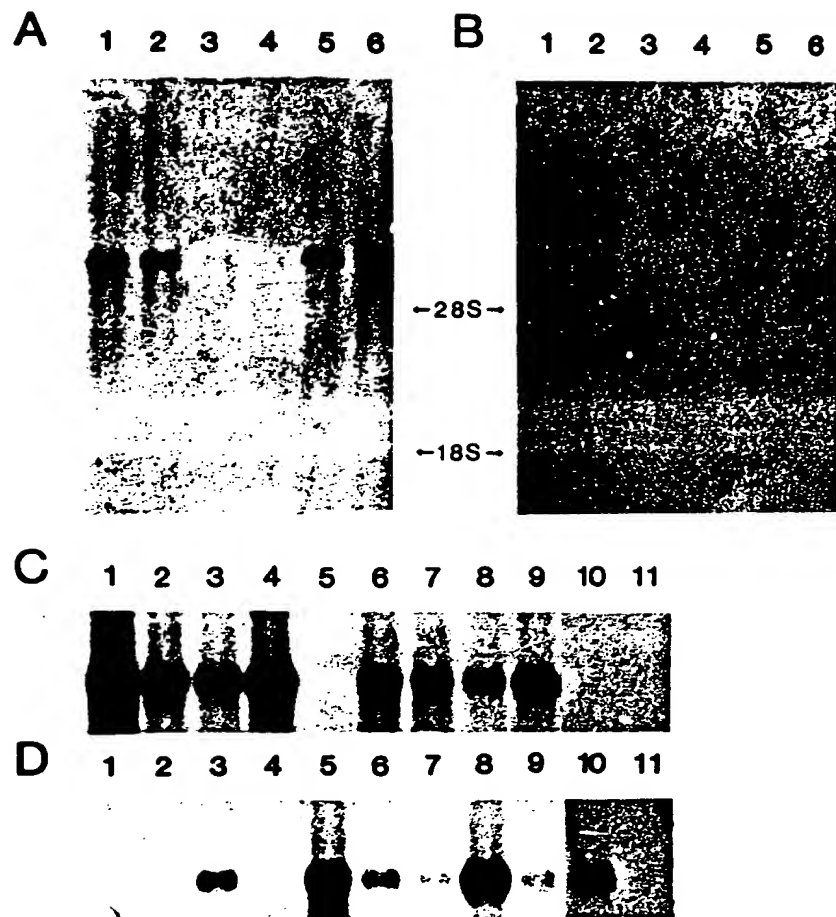Figure 6.   See Legend on next page.

79

Figure 6.   Comparison of mRNA species of the T11
and known PDGF-R genes, in normal and tumor
cells.   The same filter was first hybridized with
the probe from pT11-HP (0.95-kbp *Hind*III-*Pst*I

5   genomic fragment) (A) and then rehybridized with
a PDGF-R cDNA probe (B).   A different filter was
first hybridized with T11 cDNA (3.5-kbp *Bam*HI
fragment of TR4 including the whole coding
region) (C) and then rehybridized with PDGF-R

10   cDNA (3.8-kbp *Nde*I fragment of HPR2) (D).   A and B
contained poly (A)+ RNAs (5 µg per lane)
extracted from human smooth muscle (lane 1),
heart (lane 2), liver (lane 3), spleen (lane 4)
or embryo (lanes 5 and 6).   C and D contained

15   total RNA (20 µg per lane) extracted from G402
leiomyoblastoma cells (lane 1), SK-LMS-1
leiomyosarcoma cells (lane 2),   A1186 or A204
rhabdomyosarcoma cells (lanes 3 and 4), 8387
fibrosarcoma cells (lane 5), astrocytoma tissues

20   (lanes 6 and 7), A1690 astrocytoma cells (lane
8), A1207 or A172 glioblastoma cells (lanes 9 and
10) or A875 melanoma cells (lane 11).   Migrations
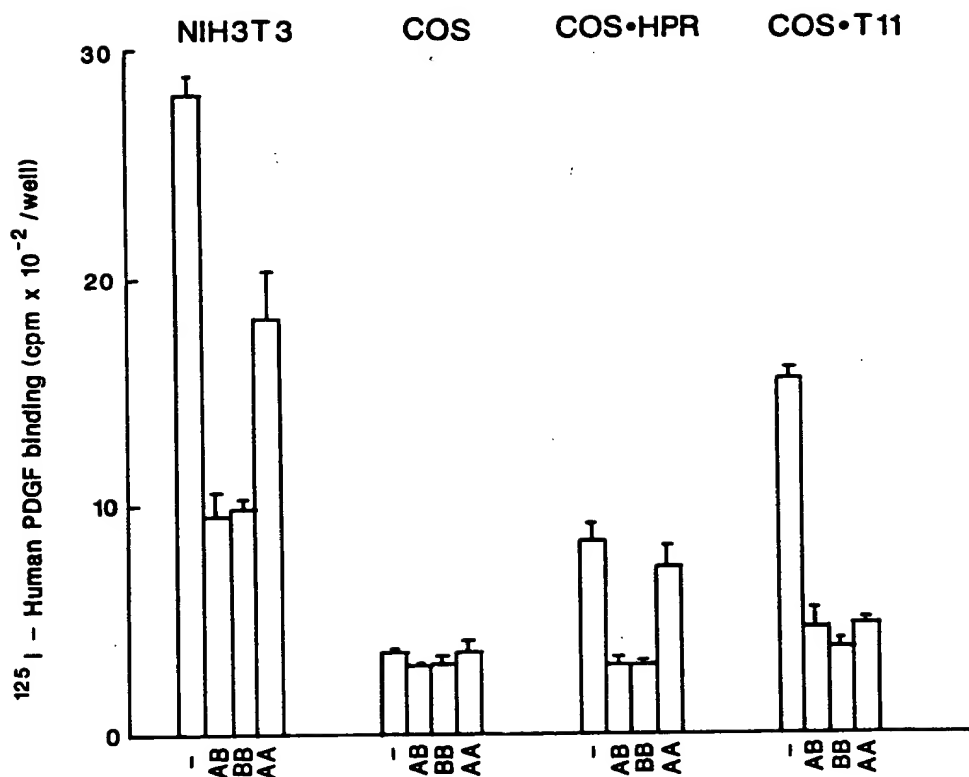of 28S and 18S ribosomal RNA (markers) are as
indicated.

Figure 7. Detection of T11 and PDGF-R proteins with peptide antisera in human cell lines (A) and COS-1 cell transfectants (B). (A) M426 human embryo fibroblasts (lanes 1, 4, 7 and 10), 8387 fibrosarcoma cells (lanes 2, 5, 8 and 11), A204 rhabdomyosarcoma cells (lanes 3, 6, 9 and 12), (B) COS-1 cells (lanes 1 and 4), COS-1 cells transfected with vectors carrying T11 cDNA (lanes 2 and 3) or PDGF-R cDNA (lanes 5 and 6).

Figure 8. Binding of ^{125}I-labeled human PDGF to mouse control NIH/3T3, control COS-1 and COS-1 cells transfected with T11 or known PDGF-R cDNA expression vectors. Results represent the mean values (±SD) of triplicate samples.
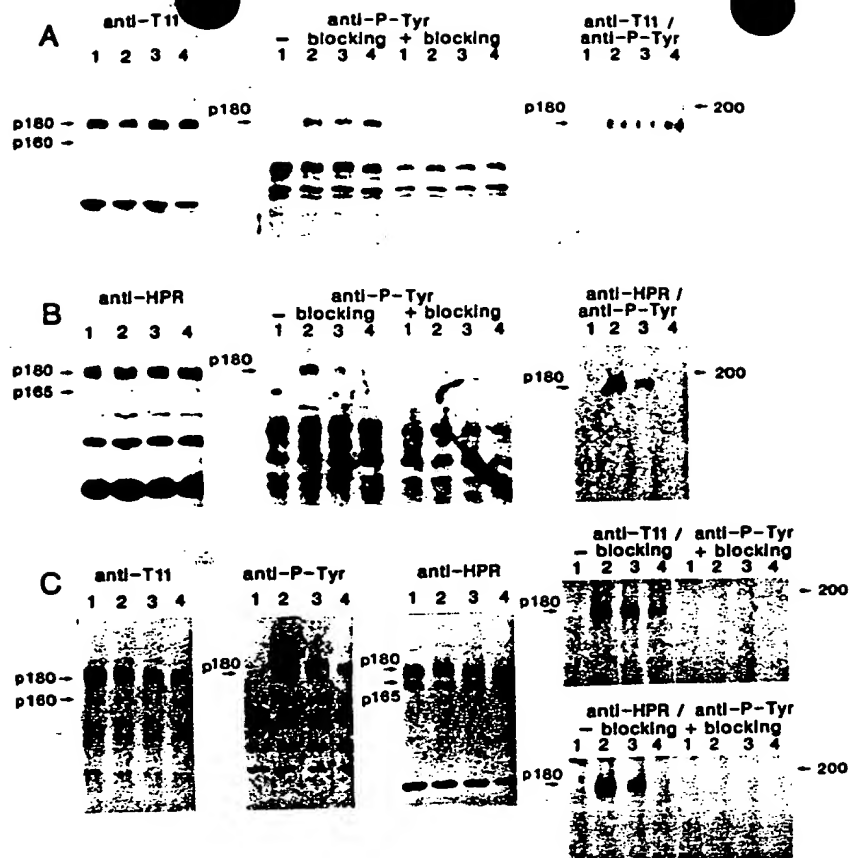
Figure 9. Tyrosine autophosphorylation of type α and type β PDGF-R gene products induced by different PDGF isoforms. A204 (A), 8387 (B), or NIH/3T3 (C) cells were incubated with PDGF-BB (30 ng/ml) (lane 2), human PDGF (30 ng/ml) (lane 3), PDGF-AA (300 ng/ml) (lane 4) or 3 mM acetic acid (vehicle control: lane 1). Cell lysates were immunoprecipitated with peptide antisera directed against predicted type α or type β PDGF receptors (anti-T11 and anti-HPR, respectively). Immunoblot analyses was with antibodies to the receptors or phosphotyrosine (anti-P-Tyr) (54) as indicated above the blots. Arrows indicate the specific bands which were blocked in the presence of immunizing peptide.
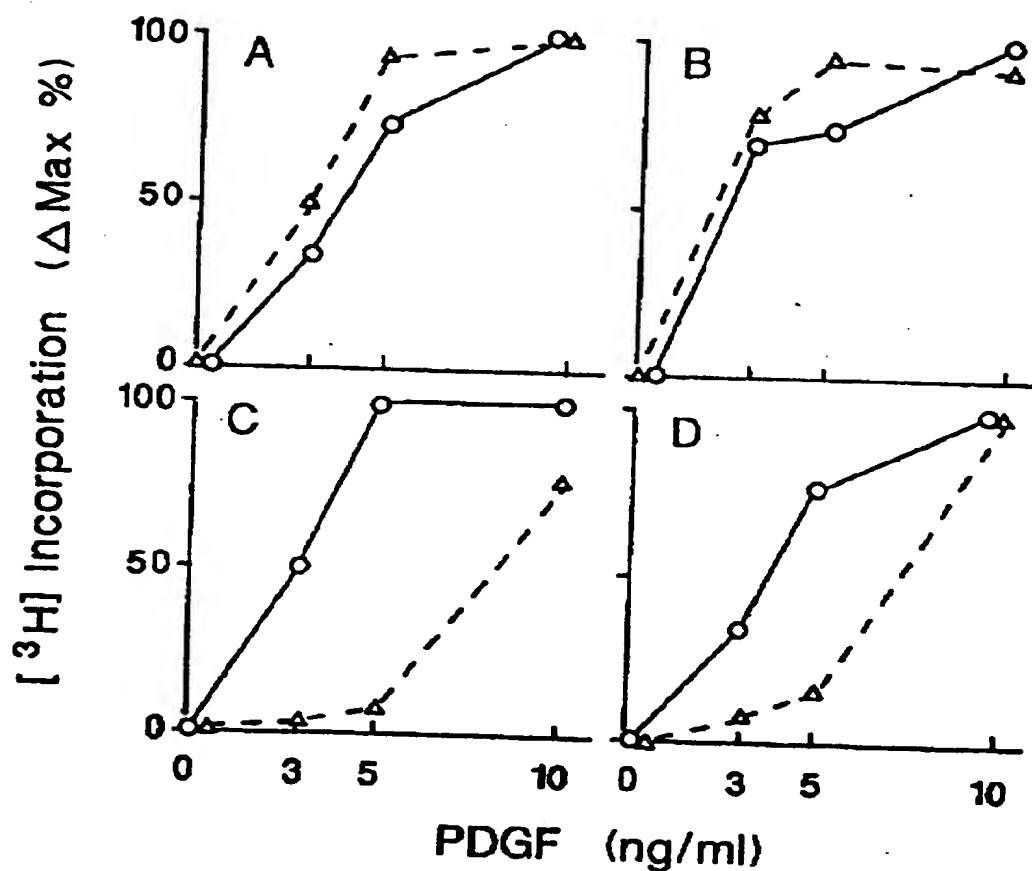
Figure 10. Stimulation of DNA synthesis
by PDGF-AB (triangles) or PDGF-BB (circles) in
various cells, as follows: (A) mouse NIH/3T3;
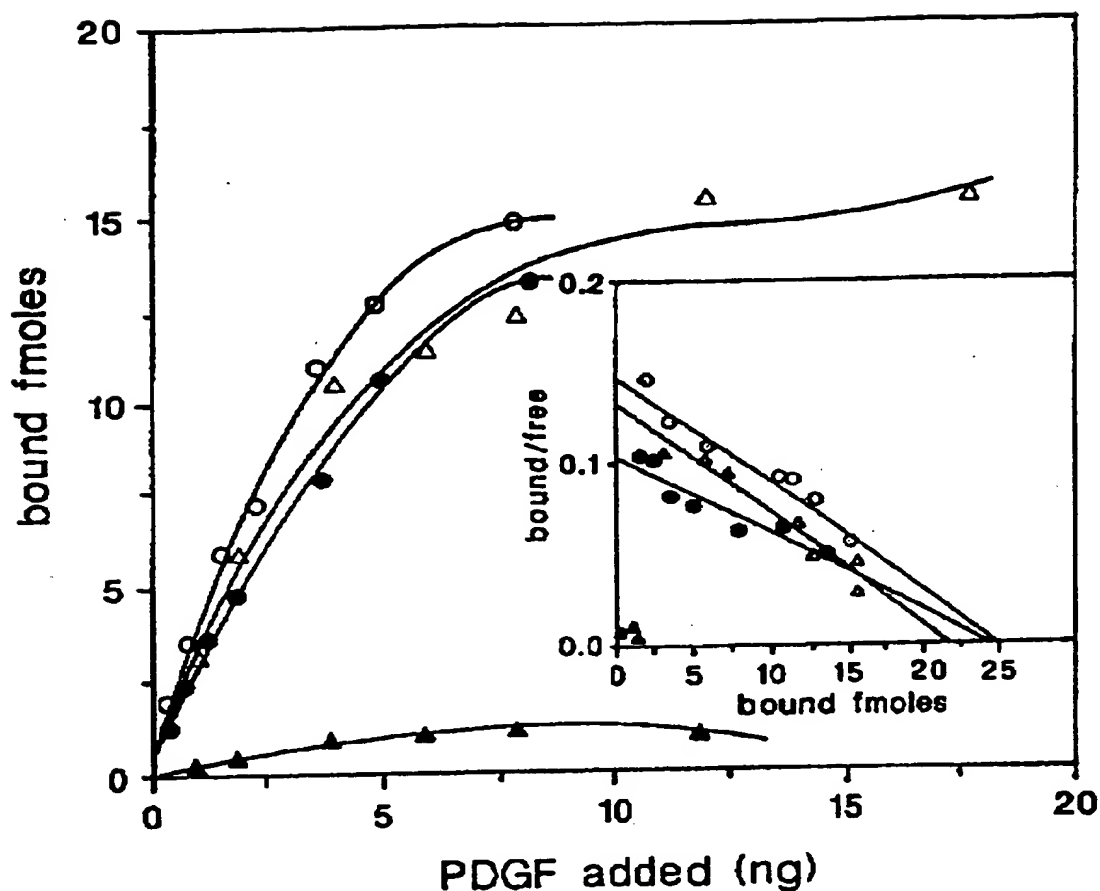(B) human M426; (C) human AG1523; (D) human M413.

Figure 11. Receptor binding of PDGF-AB (triangles) or PDGF-BB (circles) by human D32 cells reconstituted with type α (open symbols) or type β (filled symbols) PDGF receptors by transfection with vectors bearing the respective cDNAs. The inset displays the same data replotted in the standard (semi-log) Scatchard format.
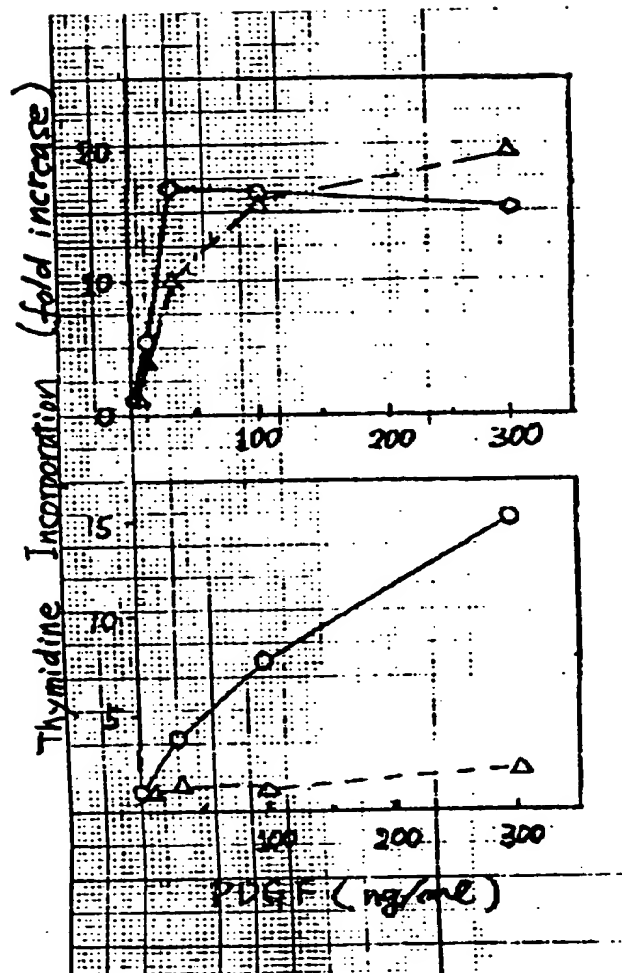
85

Figure 12. DNA synthesis stimulation responses to PDGF-AB (triangles) or PDGF-BB (circles) by human D32 cells reconstituted with type α (upper panel) or type β (lower panel) PDGF receptors.
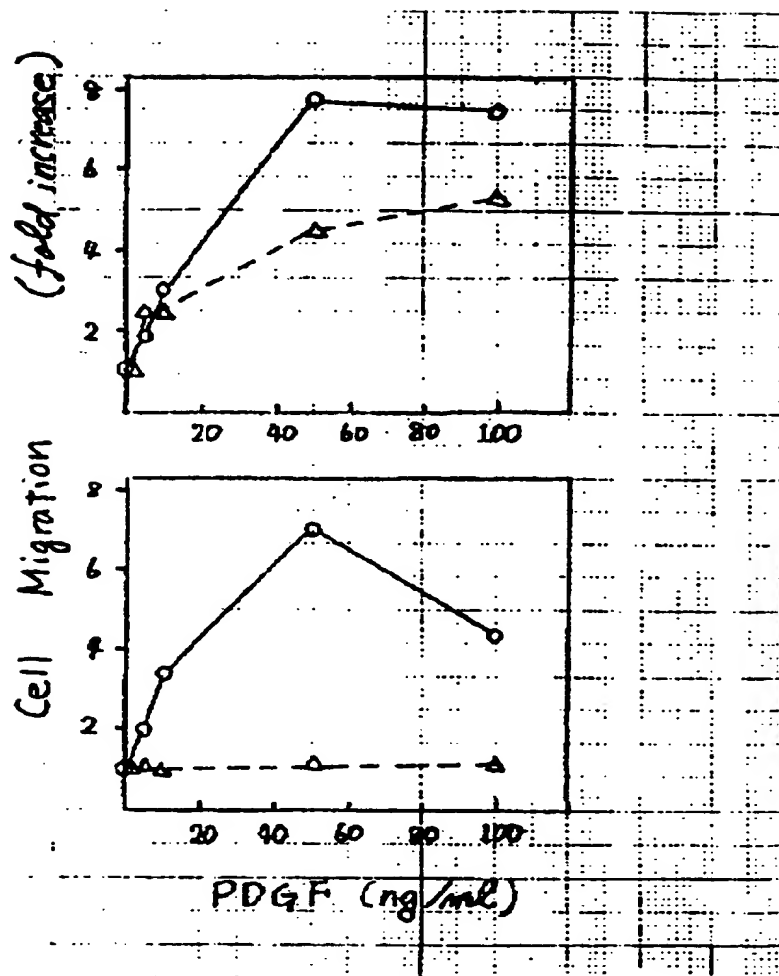
Figure 13. Chemotaxic responses to PDGF-AB (triangles) or PDGF-BB (circles) by human D32 cells reconstituted with type α (upper panel) or type β (lower panel) PDGF receptors.
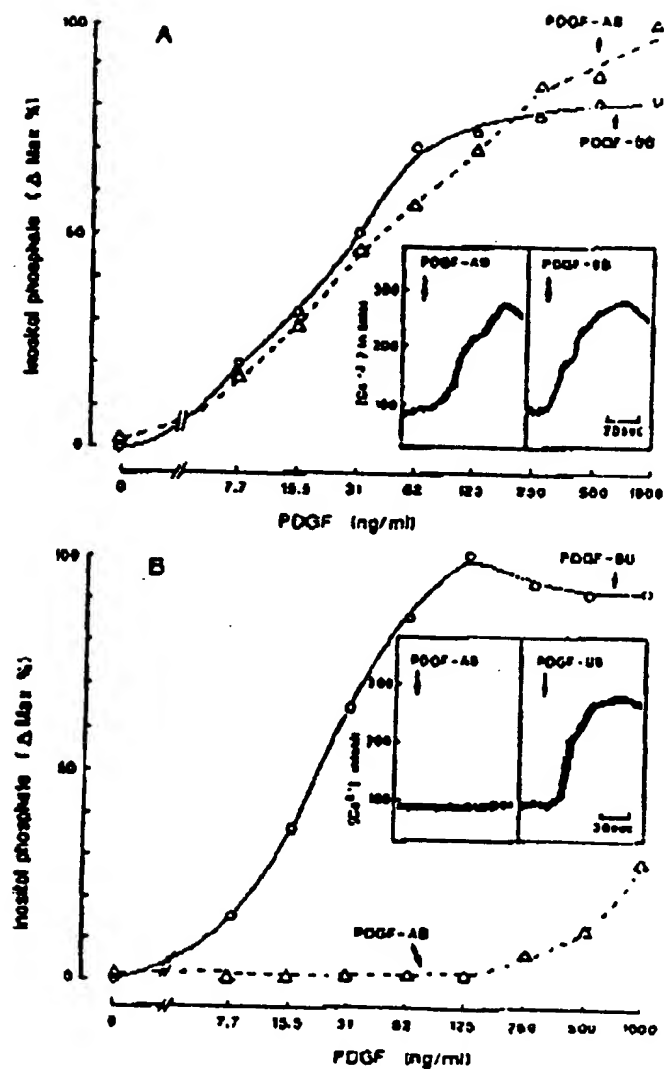
87

Figure 14. Responses of inositol phosphate formation and cytosolic calcium ion mobilization (i.e., [Ca²⁺]i; data in insets) to PDGF-AB (triangles) or PDGF-BB (circles) by human D32 cells reconstituted with type α (upper panel) or type β (lower panel) PDGF receptors.